Electrospray Ionization Based Methods for the Generation of Polynuclear Oxo- and Hydroxo Group 6 Anions in the Gas-Phase

Rosa Llusar[a,]* Ivan Sorribes[a] and Cristian Vicent[b,*]

[a] *Departament de Química Física i Analítica, Universitat Jaume I, Avda. Sos Baynat s/n, E-12071, Castelló, Spain*
[b] *Serveis Centrals d´Instrumentació Cientifica, Universitat Jaume I, Avda. Sos Baynat s/n, E-12071 Castelló, Spain*

AUTHOR EMAIL ADDRESS:
* author for correspondence: ; Rosa.Llusar@qfa.uji.es ; barrera@sg.uji.es

RUNNING HEAD:
gas-phase ion chemistry of group 6 oxo- and hydroxo anions

Abstract

Electrospray ionization (ESI) of the Lindqvist $(n\text{-}Bu_4N)_2[M_6O_{19}]$ (M = Mo, W) polioxometalates provides a straightforward entry for the generation of an assortment of oxo- and hydroxo anions in the gas-phase. In particular, the series of oxo dianions of general formula $[(MO_3)_nO]^{2-}$ (n = 2-6; M = Mo, W), monoanions, namely $[(MO_3)_nO]^-$ (n = 1, 2) and $[(MO_3)_n]^-$ (n = 1, 2), and the hydroxo $[(MO_3)_n(OH)]^-$ (n = 1-6) species can be readily generated in the gas-phase upon varying the solvent composition as well as the ionisation conditions (typically the U_c cone voltage). Complementary tandem mass experiments (collision induced dissociation and ion-molecule reactions) are also used aimed to investigate the consecutive dissociation of these species and their intrinsic gas-phase reactivity towards methanol. Special emphasis is paid to some of the key factors of these group 6 anions related to the gas-phase activation of methanol, such as molecular composition, open vs closed shell electronic nature and cluster size.

Keywords: group 6 oxide anions; hydroxo complexes; Electrospray ionization, CID, ion-molecule reactions

1. Introduction

Group 6 oxides are employed in a variety of industrial catalytic reactions that includes the selective oxidation of alcohols to aldehydes over Fe:MoO_3 surfaces[1] and the isomerization of alkanes using tungsten or molybdenum oxides.[2] Besides metal-oxo M=O functional groups, metal-hydroxo M-OH fragments are also important intermediates in many catalytic processes occurring at metal oxide surfaces.[1,3] For example, the ability of oxo-metal fragments to activate C-H or O-H bonds of organic substrates and to form a metal-hydroxo fragment is crucial to their catalytic function in many chemical, industrial and biological processes.[4] However, the details of the molecular mechanism of many reactions occurring at the oxide surfaces during the catalytic processes are not yet fully understood in part due to the complexity of the catalyst surface and also to the possibility of different reaction sites. In this context, mass spectrometric techniques have emerged as a promising approach to obtain fundamental insight into isolated molecules in the gas-phase which can aid in the interpretation of the complicated structures and chemical processes occurring at the oxide surfaces.[5-12] In particular, the study of group 6 oxide anions in the gas-phase has been extensively investigated using different ion production techniques. The sputtering of MoO_3 using the fast atom bombardment (FAB) technique yielded the $[MoO_n]^-$ (n = 2-4) and $[Mo_2O_n]^-$ (n = 4, 5) ions.[13] Thermal desorption has also been employed as a means of generating the series of group 6 oxide $(MoO_3)_n^-$ (n = 1-13) and $(WO_3)_n^-$ (n = 1-8) anions.[14]

In the last decade, the use of laser evaporation techniques has been dominant for the gas-phase production of group 6 oxide clusters.[13,15-17] As illustrated in the gas-phase generation of $[(MO_3)_n]^-$ or $[(MO_3)_nO]^-$ (n = 1,6; M = Mo, W),[18,19] laser evaporation techniques typically generate an assortment of oxo-clusters with different stoichiometries and nuclearities. Complementary experimental techniques, such collision induced dissociation (CID) or ion-molecule reactions, in conjunction with computational methods are employed to get deep insight on the electronic and structural characterics of the generated gas-phase species. In parallel with these reactivity studies, gas-phase investigations using photoelectron spectroscopy (PES) provide information about the electronic and geometric structure of metal oxide species, which is also relevant for understanding the reactivity and catalytic function of these and other related species.[20-26]

Electrospray ionisation (ESI) mass spectrometry represents another versatile approach to study the gas-phase ion chemistry of cluster group 6 oxo-complexes. ESI is a soft ionisation technique that permits transfer of ions from condensed-phases to the gas-phase with minimal fragmentation and has been shown to be a convenient tool for the characterization of high nuclearity group 6 polyoxyanions and for the study of their aqueous speciation under a wide pH range.[27-32] Typically, ESI generation of gaseous anions with M=O or M-OH groups heavily relies on the availability of pre-existing polynuclear entities in solution, a fact that for example precludes the production of the elusive $[W_2O_7]^{2-}$ dianion or tri- tetra- and pentanuclear group 6 oxide species in the gas-phase. Another way to produce polynuclear oxo or hydroxo metal clusters in the gas-phase relies on the successive fragmentation of high nuclearity ions under harsh electrospray ionization conditions. Prior studies have demonstrated the utility of ESI of the $[V_6O_7(OCH_3)_{12}]$ cluster for the production of gaseous oxovanadium species ranging from tetranuclear oxo $[V_4O_{10}]^+$ and hydroxo $[V_4O_{10}H]^+$ to mononuclear $[VO]^+$ and $[VO_2]^+$ cations,[33,34] to subsequently investigate their reactivity towards methanol,[35] methane[36,37] and small alkenes.[34]

In the present study, we investigate the use of electrospray ionization (ESI) to generate gas-phase oxo- and hydroxo group 6 anions using as precursor the hexanuclear Lindqvist $(n\text{-}Bu_4N)_2[M_6O_{19}]$ (M = Mo, W) polyoxoanions. Lindqvist-type $[M_6O_{19}]^{2-}$ (M = Mo, W) dianions have been viewed as molecular models for an ideal oxide surface,[38,39] where hexanuclear units formed by six MO_6 octahedra are connected each other via edge sharing oxygen atoms, thus exhibiting an approximate O_h symmetry (see figure 1).

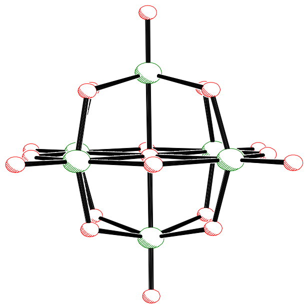

Figure 1. Schematic drawn of the Lindqvist $[M_6O_{19}]^{2-}$ polyoxoanions.

Upon harsh ESI conditions, these polyoxoanions generate an array of doubly charged gas-phase anions of general formula $[(MO_3)_nO]^{2-}$ (n = 2-6; M = Mo, W) together with singly-charged ions, namely $[(MO_3)_n]^-$ (n = 1, 2) and the $[(MO_3)_nO]^-$ (n = 1, 2) radical. Upon varying the solvent composition and the ESI conditions it is also possible to produce the series of hydroxo $[(MO_3)_n(OH)]^-$ (n = 1-6) anions. These anions might be considered as simple models for metal-oxo and metal-hydroxo fragments present at oxide surfaces, and so the present study aims to analyze their reactivity toward methanol in an attempt to possibly divulge some mechanistic information on the reactions occurring at metal oxide surfaces. In particular, the factors that may affect the reactivity including composition, electronic closed vs open-shell character and cluster size, are also addressed herein.

2. Experimental

2.1. *General Procedures*

Compounds $(n\text{-}Bu_4N)_2[Mo_6O_{19}]$[40] and $(n\text{-}Bu_4N)_2[W_6O_{19}]$[41] were prepared according to literature procedures. Acetonitrile (HPLC grade, 99.8 %), methanol (HPLC grade, 99.8 %) and formic acid were obtained from Aldrich and used without further purification.

2.2 Mass Spectrometry

Electrospray ionization (ESI) mass experiments were conducted on a Quattro LC (quadrupole-hexapole-quadrupole) spectrometer. Sample solutions were infused via syringe pump directly connected to the ESI source at a flow rate of 10 µL/min. The desolvation gas as well as nebulization gas was nitrogen at a flow of 450L/h and 80 L/h respectively. A capillary voltage of 3.3 kV was used in the negative scan mode. The cone voltages (U_c) applied in the cone region of the differentially pumped ESI source were systematically varied for the analysis of $(n\text{-}Bu_4N)_2[M_6O_{19}]$ (M = Mo, W), typically in the U_c = 30-190 range in order to analyse their characteristic ¨in-source¨ dissociation. Related experiments using a Q-TOF I (quadrupole-hexapole-time-of-flight) tandem mass spectrometer operating at a resolution of 5000 FWHM, were also carried out to unambiguously confirm the charge-state of the detected species. In order to investigate the consecutive gas-phase dissociation of the array of oxo- and hydroxo group 6 anions, collision induced dissociation (CID) experiments were also studied. For CID spectra, the anions of interest were mass-selected using the first quadrupole (Q1) and interacted with argon in the hexapole collision cell under multiple-collision conditions (typically 7×10^{-4} mbar) at variable collision energies (CE = 0-30 eV) while scanning Q2 to monitor the ionic products of fragmentation. An isolation width of 1 Da was used in the first quadrupole analyser.

Ion-molecule reactions were carried out by mass-selection of the desired group 6 oxo- and hydroxo anions by means of Q1 and interacted with CH_3OH in the hexapole operating in the RF-only mode, while scanning Q2 to monitor the newly formed ionic fragments. An isolation width of 1 Da was used in Q1 and the collision energy in the hexapole collision cell was nominally set to a value of CE = 0 eV to increase the residence time of the ions in the collision cell and to ensure that reactions take place at or near thermal energies. The neutral volatile substrates were introduced in the collision cell as a part of the collision gas at a pressure in the collision cell maintained at approximately 2×10^{-4} mbar.

3. Results and discussion

Gas-phase synthesis of group 6 oxo anions

In the present work, ESI mass spectrometry of the $(n\text{-}Bu_4N)_2[M_6O_{19}]$ (M = Mo, W) complexes is investigated to generate an array of mono-, di-, tri-, tetra- and pentanuclear group 6 oxide anions as gas-phase species. Minor differences regarding the identity of the Mo and W species detected upon ESI of the Lindqvist $(Bu_4N)_2[M_6O_{19}]$ polyoxoanions were observed, so ESI studies of both group 6 anions are described together along the text. Negative ESI mass spectra of acetonitrile solutions of $(Bu_4N)_2[M_6O_{19}]$ recorded at gentle conditions (typically at U_c below 30 V) yield, as previously reported, the corresponding $[M_6O_{19}]^{2-}$ (M = Mo, W) dianions as base peak.[27,42] Figure 2 illustrates the ESI mass spectra of the $(n\text{-}Bu_4N)_2[W_6O_{19}]$ salt recorded at different cone voltages. When the cone voltage is increased within the U_c = 30-90 V range (see figure 2 middle), the $[W_6O_{19}]^{2-}$ dianion (m/z = 704) begins to dissociate due to termolecular collisions occurring in the cone region to afford the series of smaller polyoxoanions of general formula $[(WO_3)_nO]^{2-}$ (n = 3, 4, 5) down to the dinuclear $[W_2O_7]^{2-}$ species. The penta- and tetranuclear dianions $[W_5O_{16}]^{2-}$ (m/z = 588) and $[W_4O_{13}]^{2-}$ (m/z = 472) are both observed as minor species in the U_c = 30-90 V range, whereas the trinuclear $[W_3O_{10}]^{2-}$ dianion (m/z = 356) is the dominant species from U_c = 30 to 90 V. Related ESI mass spectra were recorded with the Q-TOF I instrument operating at a resolution of ca. 5000 FWHM to further confirm the charge state of each detected dianion. When ionization conditions are further enforced (U_c above 120 V) (see figure 2 top), prominent signals attributed to single-charged dimers, namely $[W_2O_7]^-$ (m/z = 480) and $[W_2O_6]^-$ (m/z = 464) and monomers $[WO_4]^-$ (m/z = 248) and $[WO_3]^-$ (m/z = 232) are observed. Identical species are also seen for the Mo homologue at nearly the same cone voltage used for the generation of the W-containing anions.

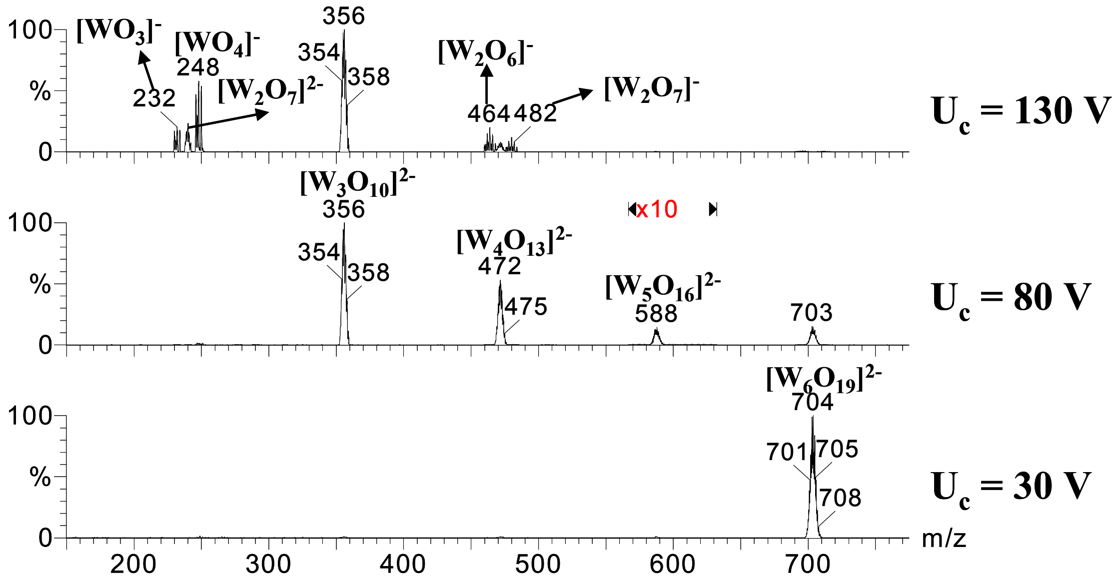

Figure 2. ESI mass spectra of acetonitrile solutions of $(Bu_4N)_2[W_6O_{19}]$ recorded at gentle ionization conditions (U_c = 30 V) (bottom), U_c = 80 V (middle) and U_c = 130 V (top). Note that the signal corresponding to the $[W_5O_{16}]^{2-}$ dianion has been ten-fold increased.

Insert table 1

Table 1 lists the different species generated by ESI starting from the Lindqvist $(Bu_4N)_2[M_6O_{19}]$ (M = Mo, W) polyoxoanions upon different experimental conditions. Other generation sources used for the production of gaseous group 6 anions such as laser evaporation or fast atom bombardment (FAB) techniques invariably lead to the formation of monanionic species.[13,18,21,24] Our work illustrates the potential of electrospray ionization to transfer multiple-charged species to the gas-phase, such as the complete $[(MO_3)_nO)]^{2-}$ (n = 2-6; M = Mo, W) series (see entries 1-5 in table 1). In addition, the series of singly-charged anions $[(MO_3)_nO]^-$ and $[(MO_3)_n]^-$ (M = Mo, W; n = 1, 2) can also be easily generated in the gas-phase by cluster degradation of $[M_6O_{19}]^{2-}$ dianions upon harsh ESI conditions (entries 6-9 in table 1), thereby offering an alternative to the widespread application of laser evaporation techniques for the production of these species.[19,20,22,25,43] As we shall show below, it is also possible to produce group 6 oxides featuring hydroxo groups (see entries 10-14 in table 1) by using ESI methods. In this sense it is worth pointing out that gas phase ion chemistry of hydroxo group 6 species has been scarcely explored, despite their crucial role as intermediates in the catalytic processes involving methane or methanol oxidation reactions over metal oxide surfaces. To the best of our knowledge, the production of gaseous mono- $[MO_3(OH)]^-$ and dinuclear $[M_2O_5(OH)]^-$ and $[M_2O_6(OH)]^-$ (M = Mo, W) anions is restricted to ESI methods which has allowed to explore their intrinsic reactivity towards alcohols.[44-46]

In order to investigate the consecutive fragmentation behaviour of $[M_6O_{19}]^{2-}$ in more detail, we carried out collision induced dissociation (CID) experiments on mass-selected $[(MO_3)_nO]^{2-}$ (M = Mo, W; n = 2-6) dianions. A common feature of the gas-phase dissociation of the $[(MO_3)_nO]^{2-}$ (n = 4-6) dianions is the dominant formation of the trinuclear $[M_3O_{10}]^{2-}$ species in the CE range studied. For example, upon CID of the $[M_6O_{19}]^{2-}$ (M = Mo, W) dianion at CE = 15 eV, the dominant peak is still the mass-selected $[M_6O_{19}]^{2-}$ dianion, the relative intensity of the $[M_5O_{16}]^{2-}$ and $[M_4O_{13}]^{2-}$ species represents the 2 and 15 %, respectively whereas the relative abundance of the $[M_3O_{10}]^{2-}$ dianion is 30 %. At CE = 30 eV, the exclusive presence of the trinuclear $[M_3O_{10}]^{2-}$ dianion is observed. CID spectra closely parallels ¨in-source¨ dissociation spectra of the $[M_6O_{19}]^{2-}$ dianion in which the $[M_5O_{16}]^{2-}$ and $[M_4O_{13}]^{2-}$ species are never the base peak in the ESI spectra in the U_c range investigated. Scheme 1 illustrates the consecutive dissociation pattern of the series of $[(MO_3)_nO]^{2-}$ (n = 2-6) dianions.

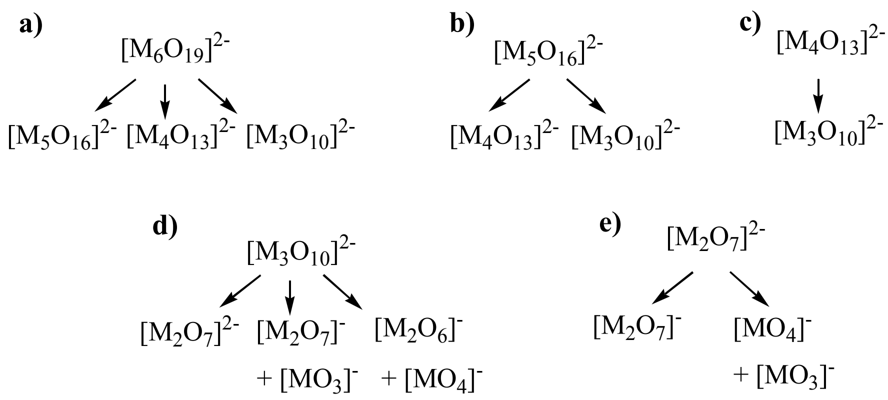

Scheme 1

CID spectra of $[M_5O_{16}]^{2-}$ consist in the expulsion of M_2O_6 fragments to afford the $[M_3O_{10}]^{2-}$ dianion as the dominant product ion together with minor amounts of $[M_4O_{13}]^{2-}$ as a result of the MO_3 liberation (see scheme 1 b) whereas CID spectra of $[M_4O_{13}]^{2-}$ exclusively release MO_3 fragments to afford the trinuclear $[M_3O_{10}]^{2-}$ dianion (see scheme 1 c). These experimental evidences suggest that the gas-phase formation of $[M_5O_{16}]^{2-}$ and $[M_4O_{13}]^{2-}$ dianions is energetically unfavoured in front of that of the trinuclear $[M_3O_{10}]^{2-}$ dianion. Let us note that with the present experiments it is not possible distinguish whether the liberated neutral fragments corresponds to the sequential loss of MO_3 oxide units or the cleavage of single M_2O_6 or M_3O_9 (or M_2O_6 + MO_3) units. The CID spectra of mass-selected $[M_3O_{10}]^{2-}$ and $[M_2O_7]^{2-}$ (M = Mo, W) dianions are shown in figure 3.

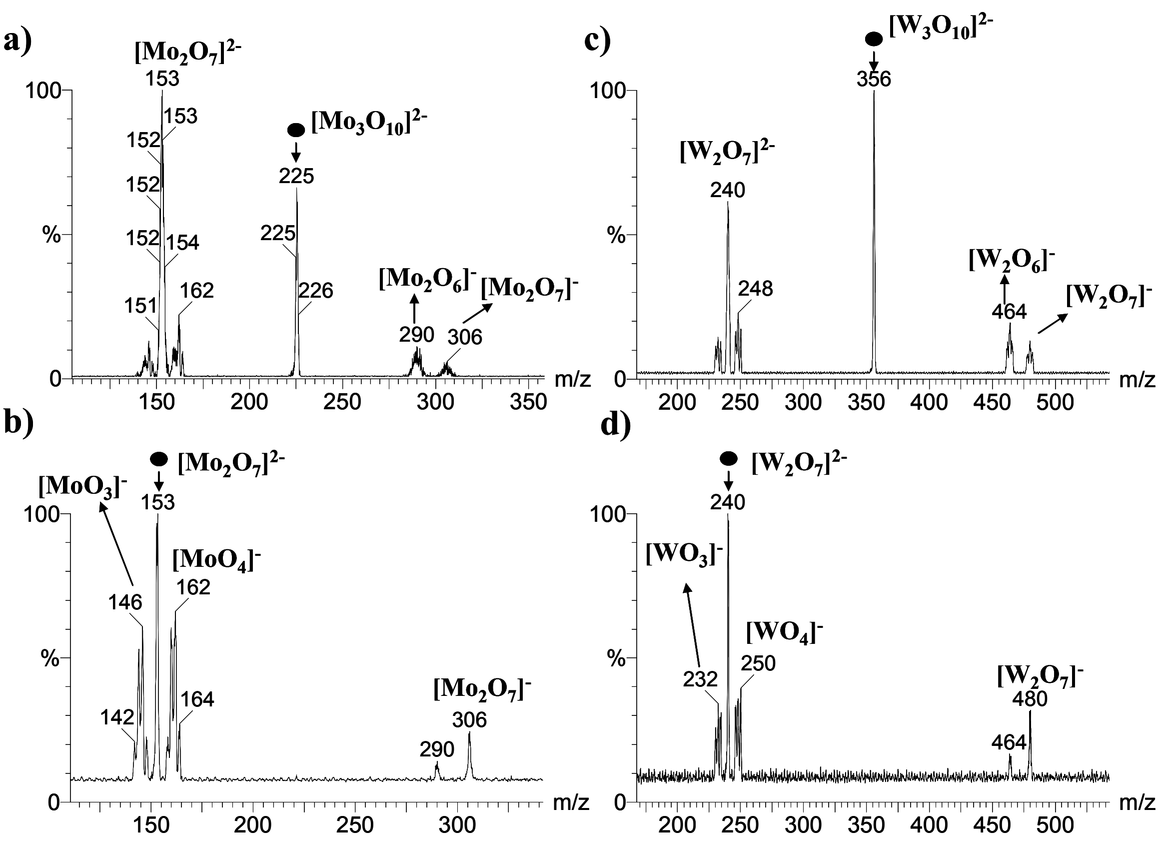

Figure 3. CID spectra at CE = 20 eV of mass selected a) $[Mo_3O_{10}]^{2-}$ (m/z = 225); b) $[Mo_2O_7]^{2-}$ (m/z = 153); c) $[W_3O_{10}]^{2-}$ (m/z = 356) and d) $[W_2O_7]^{2-}$ (m/z = 240)

CID spectra of mass-selected $[M_3O_{10}]^{2-}$ dianion comprises up to three different dissociation channels according to scheme 1 d. Besides the ubiquitous liberation of MO_3 fragments to afford the $[M_2O_7]^{2-}$ dianion, dissociation through ionic fragmentation is also observed to yield the $[M_2O_6]^-$ and $[M_2O_7]^-$ monoanions concomitant with the formation of $[MO_4]^-$ and $[MO_3]^-$, respectively. CID spectra of the $[M_2O_7]^{2-}$ dianion is significantly different from those found for the series of larger $[(MO_3)_nO]^{2-}$ (n = 3, 4, 5, 6) dianions where the formal dissociation of MO_3 fragments is not observed at all. Instead, mass-selection and CID of $[M_2O_7]^{2-}$ exclusively produces $[MO_3]^-$ and $[MO_4]^-$ through ionic dissociation together with the product ion $[M_2O_7]^-$ formed through electron-detachment according to scheme 1 e.

Qualitative thermochemical information on the preferred dissociation pathways in multiply charged dianions can be extracted from these low-energy CID experiments. Firstly, we observe that the fragmentation pathways for the $[(MO_3)_nO]^{2-}$ (n = 2-6) dianions are strongly dependent on the cluster size, an observation that can be rationalized on the basis of the enhanced intramolecular Coulomb repulsion as the molecular size of the multiply charged anion is reduced. For example, CID of the $[(MO_3)_nO]^{2-}$ (M = Mo, W; n = 4-6) dianions produce formal losses of MO_3, M_2O_6 or M_3O_9 fragments while retaining the initial charge state, therefore suggesting that the energy of Coulomb repulsion is smaller than that involving M-O chemical bonds. For $[M_6O_{19}]^{2-}$ dianions, intramolecular Coulomb repulsion is estimated to be about 2 eV.[42] As the cluster size of the dianion is reduced, namely $[M_3O_{10}]^{2-}$ (M = Mo, W) additional dissociation pathways compete with the MO_3 liberation that involve ionic fragmentation processes (see figure 3 a and c). That means that the energy of Coulomb repulsion in $[M_3O_{10}]^{2-}$ (M = Mo, W) is similar to the chemical bond strength associated to the ionic fragmentation. For the smaller $[M_2O_7]^{2-}$ dianions, strong intramolecular Coulomb repulsion make them prone to decay via either ionic fragmentation or electron detachment while the expulsion of MO_3 fragments (that formally would lead to the unstable $[MO_4]^{2-}$ dianion) is not observed. As can be inferred from figure 3 b and d, the relative abundance of the product ions formed from electron-detachment and ionic fragmentation processes are comparable, thus suggesting that both processes are associated to similar energetic barriers. The gas-phase dissociation of the chromium $[Cr_2O_7]^{2-}$ homologue generated by ESI has been recently reported to yield identical monoanionic product ions, namely $[Cr_2O_7]^-$, $[CrO_4]^-$, and $[CrO_3]^-$. For the $[Cr_2O_7]^{2-}$ dianion, the energetic barrier for the ionic fragmentation is higher that that involving electron-detachment, an observation attributed to the strong covalent Cr-O bonding within this anion.[47]

The observation of $[MO_4]^-$ and $[M_2O_7]^-$ (M = Mo, W) is remarkable from an oxidation state perspective, because the formal oxidation state is 7 for the metal in the mononuclear anions whereas an average value of 6.5 is calculated for the dinuclear ions. Since oxidation states of M beyond 6 are unlikely, these species must be formulated as radicals, or as peroxy structures. In general, the gas-phase dissociation of these radical $[M_2O_7]^-$ and $[MO_4]^-$ species is governed by the formal expulsion of neutral oxygen to afford $[M_2O_6]^-$ and $[MO_3]^-$, respectively as illustrated in scheme 2 a and b. CID of $[M_2O_7]^-$ also revealed the liberation of MO_3 fragments to produce $[MO_4]^-$.

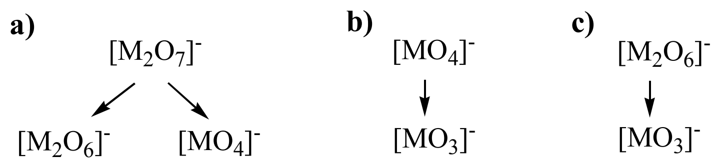

Scheme 2

Regarding the monoanions $[M_2O_6]^-$ and $[MO_3]^-$, they do not readily fragment by low-energy CID and their intensity markedly decrease with increasing CID energy, thus suggesting that electron detachment is occurring. The only process experimentally observed for $[M_2O_6]^-$ was elimination of minor amounts of MO_3 to yield $[MO_3]^-$.

Gas-phase synthesis of group 6 hydroxo anions

Our approach for the production of group 6 hydroxo anions in the gas-phase relies on the ubiquitous fragmentation of large polyoxoanions through the liberation of MO_3 fragments. Hence, we explore the possibility to transfer the corresponding hexanuclear hydroxo $[M_6O_{18}(OH)]^-$ (M = Mo, W) anion to the gas-phase to subsequently dissociate it to afford an array of smaller hydroxo $[(MO)_3(OH)]^-$ (n = 1, 6) anions. For this purpose, the ESI mass spectra of acetonitrile/formic acid solutions of complexes $(n\text{-}Bu_4N)_2[M_6O_{19}]$ (M = Mo, W) were investigated. Under gentle conditions (U_c = 30 V) the negative ESI mass spectra show, besides the pseudo-molecular $[M_6O_{19}]^{2-}$ dianion, a prominent peak corresponding to the protonated $[M_6O_{18}(OH)]^-$ monoanion. The use different solvent composition, in particular formic acid:CH_3CN ratios, shows that the relative abundance of the protonated $[M_6O_{18}(OH)]^-$ anion with respect to the $[M_6O_{19}]^{2-}$ dianion increases upon increasing the formic acid:CH_3CN ratio, however significant ion suppression is observed as a consequence of the competing ionisation of formic acid in the negative ESI mass spectra. Optimal formic acid to CH_3CN ratio was found at 10:90 at which the relative ratio of $[M_6O_{18}(OH)]^-$:$[M_6O_{19}]^{2-}$ is ca 20 %. Upon more harsh ionisation conditions (typically in the U_c = 50-150 V range), liberation of neutral MO_3 fragments is observed to give rise the series of $[(MO_3)_nOH]^-$ (n = 1-6) anions bearing hydroxo groups. The optimum cone voltages to produce maximum abundances of each species are collected in table 1.

Like the typical low abundance observed for the group 6 oxo $[M_5O_{16}]^{2-}$ and $[M_4O_{13}]^{2-}$ (M = Mo, W) dianions, the formation of the tetranuclear $[M_4O_{12}(OH)]^-$ species was dramatically reduced and the pentanuclear $[M_5O_{15}(OH)]^-$ anion was not observed in the whole U_c range investigated, an observation that points towards an inherent unstability of these species in the gas-phase. A peculiarity of the present system arises from the fact that due to the initial coexistence of anions $[M_6O_{19}]^{2-}$ and $[M_6O_{18}(OH)]^-$ at low cone voltages, species detected upon ¨in-source¨ fragmentation indeed correspond to those resulting from both $[M_6O_{19}]^{2-}$ and $[M_6O_{18}(OH)]^-$. Consequently oxo and hydroxo mononuclear species generated at high cone voltages, namely $[MO_4]^-$ (originating from $[M_6O_{19}]^{2-}$, see scheme 1 and 2) and $[MO_3(OH)]^-$ (originating from $[M_6O_{18}(OH)]^-$, see scheme 3) are partially overlapped. Similarly, superposition is also observed for the dimers $[M_2O_7]^-$ (originating from $[M_6O_{19}]^{2-}$) and $[Mo_2O_6(OH)]^-$ (originating from $[M_6O_{18}(OH)]^-$) and therefore mass-selection of non-overlapped isotopomers is required to investigate the gas-phase ion-chemistry of these species. Additional experiments using CID further confirm the characteristic release of MO_3 fragments from the series of $[(MO_3)_n(OH)]^-$ (n = 4-6) anions. Like the series of oxo complexes described above, upon mass-selection and CID of the $[(MO_3)_n(OH)]^-$ (n = 4-6) anions, the dominant product ion was the trinuclear $[M_3O_9(OH)]^-$ species. CID spectra of mass-selected $[M_6O_{18}(OH)]^-$ show the formation of a dominant species corresponding to the $[M_3O_9(OH)]^-$ anion (through the formal liberation of M_3O_9) along with minor signals of $[M_4O_{12}(OH)]^-$ that corresponds to the expulsion of M_2O_6 fragments (see scheme 3 a).

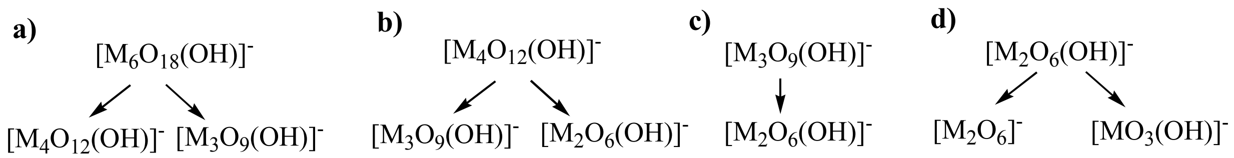

Scheme 3

CID spectra of $[M_4O_{12}(OH)]^-$ exclusively comprise the liberation of MO_3 and M_2O_6 fragments to afford the $[M_3O_9(OH)]^-$ and $[M_2O_6(OH)]^-$ anions, respectively (see scheme 3 b). CID spectra of $[M_3O_9(OH)]^-$ and $[M_2O_6(OH)]^-$ is dominated by expulsion of one MO_3 unit producing the dinuclear $[M_2O_6(OH)]^-$ and the mononuclear $[MO_3(OH)]^-$ anions, respectively. Additionally, the formal loss of an hydroxo group is observed for the dimer $[M_2O_6(OH)]^-$ as a minor fragmentation channel.

Intrinsic reactivity of group 6 oxo- and hydroxo anions towards methanol

The reactivity of the ions generated via ESI is briefly addressed in order to demonstrate the usefulness of this rather simple ESI-based method of gas-phase generation of group 6 anions. In the present work, it is remarkable the easiness to gas-phase generate an assortment of group 6 oxo anions by simply varying the cone voltage (so-called via ¨in-source¨ dissociation) or the composition of the solvent to yield group 6 polyoxoanions featuring different nuclearities (from 1 to 6), net charge (mono- or dianions) as well as electronic structure (open vs closed shell nature). Hence, the desired mass-selected anion was allowed to react with neutral substrates in the hexapole collision cell and the product ions formed were detected by scanning the second quadrupole analyser. Methanol was chosen a simple test substrate in preliminary reactivity studies. The results of the reactions between group 6 oxo- and hydroxo anions and methanol are collected in table 2.

Insert Table 2

For the series of closed-shell species, namely $[(MO_3)_nO]^{2-}$ (n = 2-6) dianions and $[(MO_3)_n]^-$ (n = 1, 2) monoanions, no significant gas-phase reactivity towards methanol is observed. For the radical $[MO_4]^-$ (M = Mo, W) anions, hydrogen abstraction according to reaction 1 is the dominant reaction channel to yield the $[MO_4H]^-$ (M = Mo, W) anions as ionic product concomitant with two possible radical species, the methoxy radical $CH_3O\cdot$ and the thermochemically more stable hydroxymethyl ($\cdot CH_2OH$) radical. Figure 4 shows the ion-molecule spectra for the reaction of mass-selected $[WO_4]^-$ and $[W_2O_7]^-$ with CH_3OH.

$$[MO_4]^- + CH_3OH \rightarrow [MO_4H]^- + [CH_3O\cdot \text{ or } CH_2OH\cdot] \qquad (1)$$

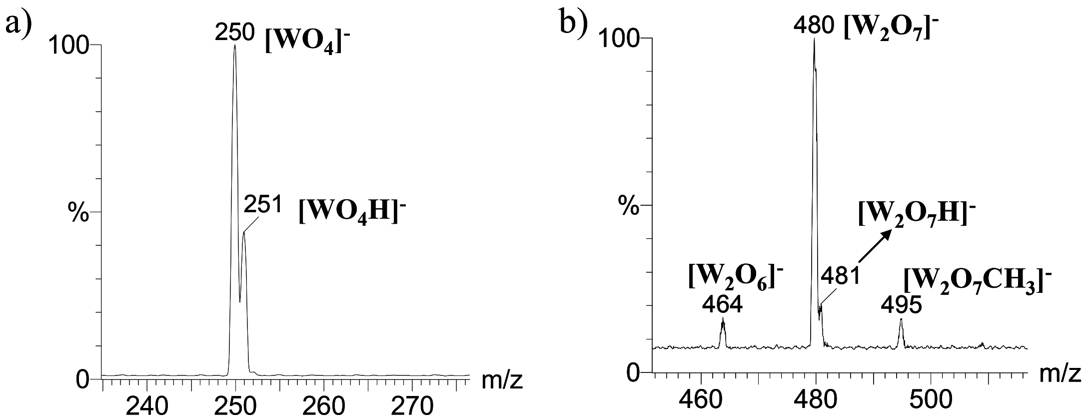

Figure 4. Reaction of CH_3OH with mass-selected a) $[WO_4]^-$ (m/z = 250) and b) $[W_2O_7]^-$ (m/z = 480).

The intrinsic reactivity towards methanol of the closely related radical $[MoO_3]^+$ cation has been previously reported and essentially yield the $[MO_3CH_3]^+$ cation via methyl abstraction,[48,49] in sharp contrast with the reactivity based on hydrogen abstraction observed for the radical $[MO_4]^-$ anions in this work. As anticipated by Wang et. al,[45,50] the high dissociation energy calculated for the $[MO_3(OH)]^-$ anions, that is $D(MO_4\text{-}H)^-$ = 107 $kcalmol^{-1}$ (Mo) and 106 $kcalmol^{-1}$ (W), suggests that the $[MO_4]^-$ anions should be capable of activating many organic molecules in the gas-phase as experimentally observed. In the present context, it has to be pointed out that hydrogen abstraction from methanol implies that the $D(MO_4\text{-}H)^-$ bond strengths are close to or even higher than those of methanol, namely $D(OHCH_2\text{-}H)$ (91.7 $kcalmol^{-1}$) or $D(CH_3O\text{-}H)$ (102.4 $kcalmol^{-1}$) in agreement with Wang´s group results.[45,50] It is also remarkable that $D(CH_3\text{-}OH)$ (91.6 $kcalmol^{-1}$) and $D(OHCH_2\text{-}H)$ bond dissociation energies are comparable; however, abstraction of the methyl group is not observed for the $[MO_4]^-$ anions most likely due its higher kinetic barrier compared with that associated to hydrogen abstraction.

The main-reactions upon mass-selection of the radicals $[M_2O_7]^-$ (M = Mo, W) in the presence of methanol were also investigated. Figure 4 b shows the mass spectra upon reaction of mass-selected $[W_2O_7]^-$ with CH_3OH. Reaction of $[W_2O_7]^-$ with CH_3OH leads to H-atom abstraction (Δm = +1, reaction 2) to yield the $[W_2O_7H]^-$ anion as ionic product. Methyl abstraction from methanol leads to the formation of $[W_2O_7CH_3]^-$ according to reaction 3 ($\Delta m = +15$). A third reaction path ($\Delta m = -16$) is assigned to the formal loss of one oxygen atom. Loss of one O atom from $[W_2O_7]^-$ may originate either from simple release of one atom to form $[W_2O_6]^-$ or from O-atom transfer to the methanol to form the corresponding oxygenated products (or most likely a mixture of CH_2O and H_2O). Branching ratios for the oxygen loss in $[W_2O_7]^-$ were measured by collision experiments with argon in the absence of methanol in the hexapole collision cell. The presence of the $[W_2O_6]^-$ fragment upon colliding $[W_2O_7]^-$ with argon is only observed at moderate collision energies (CE = 20 eV), thus suggesting the occurrence of oxygen transfer from the group 6 oxide anion to the alcohol to presumably form H_2O and CH_2O. Identical ionic products are observed for the molybdenum $[Mo_2O_7]^-$ homologue although their branching ratios were slightly different (see table 2).

$$[M_2O_7]^- + CH_3OH \rightarrow [M_2O_7H]^- + [CH_3O\cdot \text{ or } CH_2OH\cdot] \qquad (2)$$

$$[M_2O_7]^- + CH_3OH \rightarrow [M_2O_7CH_3]^- + [OH\cdot] \qquad (3)$$

$$[M_2O_7]^- + CH_3OH \rightarrow [M_2O_6]^- + CH_2O + H_2O \qquad (4)$$

The reactions of the series of hydroxo $[(MO_3)_n(OH)]^-$ (M = Mo, W; n = 1-6) anions towards methanol were also studied in order to get further insights on the effect of the cluster size on the reactivity of hydroxo group 6 species. Prior studies on the mono- and dinuclear $[MO_3(OH)]^-$ and $[M_2O_6(OH)]^-$ (M = Mo, W) anions revealed significant differences in the characteristic methanol reactivity as the cluster size varied.[44] While dimers, namely $[M_2O_6(OH)]^-$ (M = Mo, W) readily condensate methanol to yield the corresponding alkoxo species, mononuclear $[MO_3(OH)]^-$ anions were unreactive towards methanol. This distinctive reactivity towards alcohols have been interpreted in terms of the basicity of the terminal hydroxo groups (the more basic M-OH groups, the higher condensation rate) as well as their sterical hinderance.[44]

In agreement with O´Hair´s results, mononuclear $[MO_3(OH)]^-$ (M = Mo, W) anions generated in this work did no react with methanol under our experimental conditions. Likewise, the hexanuclear $[M_6O_{18}(OH)]^-$ (M = Mo, W) anions were also unreactive towards methanol. A plausible explanation for the absence of reactivity in $[M_6O_{18}(OH)]^-$ (M = Mo, W) anions relies on the prominent Brönstead acid character for these $[M_6O_{18}(OH)]^-$ (M = Mo, W) anions.[23] Moreover, the oxygen atom located in the inner cavity of the Lindqvist $[M_6O_{19}]^{2-}$ (M = Mo, W) anions may represent the most favourable protonation site, thus leaving highly hindered hydroxo groups that can also be invoked to account for the absence of reactivity for the Lindqvist $[M_6O_{18}(OH)]^-$ (M = Mo, W) anions towards methanol. However, the series of anions $[(MO_3)_n(OH)]^-$ (M = Mo, W) with n = 2, 3, 4 were all observed to condensate methanol (Δm = + 14) to formally leads the corresponding alkoxo $[(MO_3)_n(OCH_3)]^-$ (M = Mo, W; n = 2, 3) species. Figure 5 illustrates the ion-molecule reaction spectra of mass-selected $[(M_2O_6(OH)]^-$ (a and c) and $[(M_3O_9(OH)]^-$ (b and d).

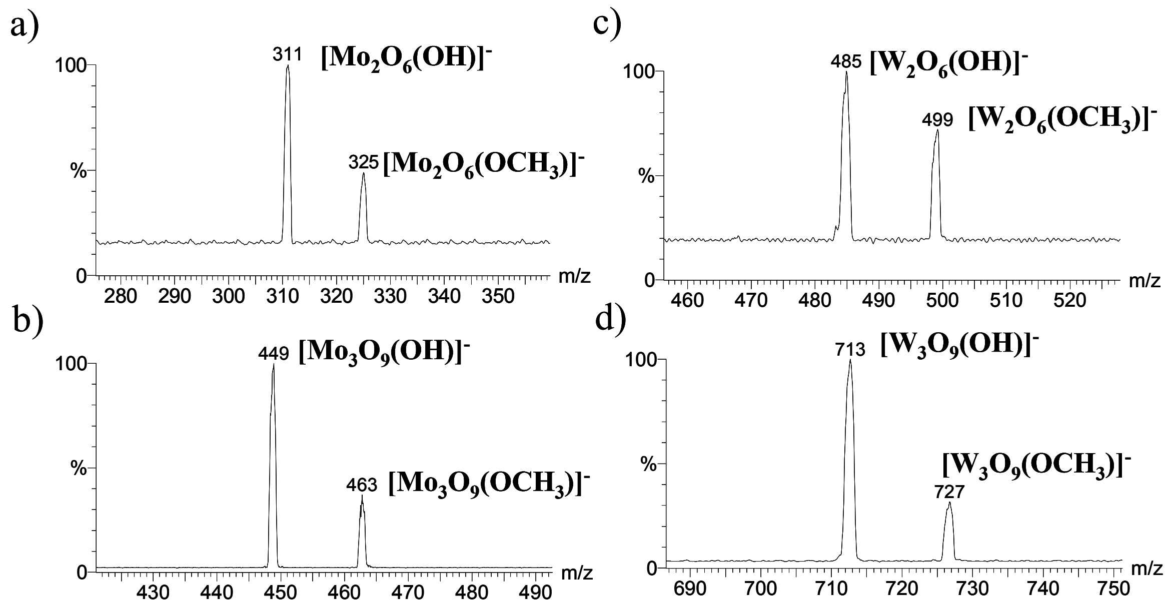

Figure 5. Reaction of CH_3OH with mass-selected a) $[Mo_2O_6(OH)]^-$ (m/z = 311); note that the isotopomer $[^{100}Mo_2O_6(OH)]^-$ was mass-selected to avoid interference from $[Mo_2O_7]^-$; b) $[Mo_3O_9(OH)]^-$ (m/z = 449); c) $[W_2O_6(OH)]^-$ (m/z = 485); note that the isotopomer $[^{186}W_2O_6(OH)]^-$ was mass-selected to avoid interference from $[W_2O_7]^-$ and d) $[W_3O_9(OH)]^-$ (m/z = 713).

For these $[(MO_3)_n(OH)]^-$ (M = Mo, W; n = 2-4) anions, it is difficult to anticipate reactivity-structure relationships because the intimate molecular organization of these species remains unknown. However, general trends can be drawn on the basis of the observed reactivity towards methanol that suggest that M-OH hydroxo groups in di-, tri- and tetranuclear species present similar basic character which is higher than that found for the mono- and hexanuclear congeners.

Conclusions

Electrospray ionisation (ESI) mass spectrometry of the Lindqvuist $(n\text{-}Bu_4N)_2[M_6O_{19}]$ (M = Mo, W) polyoxoanions allows to generate an array of group 6 oxo- and hydroxo anions. Particulary relevant is the facile tuning of the cluster distributions by variation of the solvent composition as well as the ESI conditions, thereby offering an alternative to the widespread application of laser-evaporation techniques. Collision induced dissociation (CID) experiments allows a rather comprehensive description of the product ions involved in the consecutive gas-phase fragmentation of the oxo- $[M_6O_{19}]^{2-}$ and hydroxo $[M_6O_{18}(OH)]^{2-}$ (M = Mo, W) polyoxoanions. Both Mo and W derivatives show similar dissociation patterns that can be grouped in two gas-phase dissociations types essentially determined on the cluster size of the polyoxoanion. While the larger $[(MO_3)_nO]^{2-}$ (n > 3) dianions essentially liberate neutral MO_3, M_2O_6 and M_3O_9 fragments, the smaller $[(MO_3)_nO]^{2-}$ (n = 3) dianions dissociate neutral MO_3 fragments accompanied by charge splitting processes that involves ionic fragmentation. The $[(MO_3)_nO]^{2-}$ (n = 2) dianion exclusively dissociates via charge splitting processes that involves electron-detachment as well as ionic fragmentation. This gas-phase behaviour can be interpreted in terms of the enhanced intramolecular coulomb repulsion for the dianions as the cluster size is reduced.

Ion-molecule reactions with CH_3OH, are investigated in order to unravel the fundamental reactivity of group 6 oxo- and hydroxo anions aimed at determining the molecular basis responsible for methanol activation in the gas-phase. The closed-shell oxo dianions as well as monoanions, namely

$[(MO_3)_nO]^{2-}$ (n = 2-6; M = Mo, W) and $[(MO_3)_nO]^-$ (n = 1, 2) proved to be unreactive towards methanol. However, the radical oxo species, namely $[MO_4]^-$ (M = Mo, W) readily react with methanol under thermal conditions via hydrogen abstraction to form the ionic $[MO_3(OH)]^-$ (M = Mo, W) products. In the case of the dinuclear $[M_2O_7]^-$ (M = Mo, W) radical oxo anions, besides methanol reaction through hydrogen abstraction, radical mediated methyl abstraction reactions is observed together with the formal oxygen transfer to the organic substrate (to yield H_2O and CH_2O). Regarding the group 6 hydroxo anions, distinctive reactivity towards methanol was observed as a function of the cluster size which may be ascribed to differences in the M-OH groups basicity and sterical hinderance. In particular, the molybdenum and tungsten di-, tri- and tetranuclear $[(MO_3)_n(OH)]$- (M = Mo, W; n = 2-4) promoted condensation reactions with methanol whereas the mono- and hexanuclear did not.

In summary, the radical nature and/or the cluster-size of group 6 oxo- and hydroxo anions determine the distinctive methanol cleavage in the gas-phase. A crucial factor for the modeling of group 6 oxo surfaces is the proper choice of the molecular model size; therefore, the development of approaches that allows to experimentally unraveal cluster-size effects can contribute enormously to the understanding of heterogeneous catalytic processes. Our results support recent Schwarz´s group comclusions on vanadium and aluminium oxide ions,[51,52] which state that larger systems need to be considered to properly model heterogeneous surfaces.

Acknowledgements

This work was supported by the Spanish Ministerio de Educación y Ciencia (MEC) and EU FEDER (Project CTQ2005-09270-C02-01), and Fundació Bancaixa-Universitat Jaume I (Grant P1.1B2007-12). The authors also are grateful to the Serveis Centrals d'Instrumentació Científica (SCIC) of the Universitat Jaume I for providing us with spectrometric facilities.

Table 1. Molecular formula of the group 6 oxide anions observed upon different ESI conditions and sampling cone voltages.[a]

Group 6 anions (M = Mo, W)	ESI composition / Cone voltage U_c (V)
$[M_6O_{19}]^{2-}$	CH_3CN / 30
$[M_5O_{16}]^{2-}$	CH_3CN / 50
$[M_4O_{13}]^{2-}$	CH_3CN / 50
$[M_3O_{10}]^{2-}$	CH_3CN / 90
$[M_2O_7]^{2-}$	CH_3CN / 90
$[M_2O_7]^-$	CH_3CN / 120
$[M_2O_6]^-$	CH_3CN / 120
$[MO_4]^-$	CH_3CN / 150
$[MO_3]^-$	CH_3CN / 150
$[M_6O_{18}(OH)]^-$	CH_3CN:formic acid / 40
$[M_4O_{12}(OH)]^-$	CH_3CN:formic acid / 100
$[M_3O_9(OH)]^-$	CH_3CN:formic acid / 120
$[M_2O_6(OH)]^-$	CH_3CN:formic acid / 150
$[MO_3(OH)]^-$	CH_3CN:formic acid / 150

Table 2. Branching ratios (%) for the reaction of mass-selected group 6 oxo- and hydroxo anions with methanol.

Mass-selected Group 6 anions (M = Mo, W)	$\Delta m = -16$	$\Delta m = +1$	$\Delta m = +14$	$\Delta m = +15$	$\Delta m = +32$
$[(MO_3)_n]^{2-}$ (n = 2-6)	-	-	-	-	-
$[M_2O_7]^-$	15(Mo), 30(W)	55(Mo), 40(W)	-	30(Mo), 30(W)	-
$[M_2O_6]^-$	-	-	-	-	-
$[MO_4]^-$	-	100(Mo, W)	-	-	-
$[MO_3]^-$	-	-	-	-	-
$[M_6O_{18}(OH)]^-$	-	-	-	-	-
$[M_4O_{12}(OH)]^-$	-	-	100(Mo, W)	-	-
$[M_3O_9(OH)]^-$	-	-	100(Mo, W)	-	-
$[M_2O_6(OH)]^{-,}$	-	-	100(Mo, W)	-	-
$[MO_3(OH)]^{-,}$	-	-	-	-	-

[a] Branching ratios are defined as the relative intensities of the products of ion molecule reactions normalized to $\sum = 100$.

References

1. Soares, A. P. V.; Portela, M. F. (2005), *Catal. Rev.-Sci. Eng.*, *47*, 125.
2. Ono, Y. (2003), *Catal. Today*, *81*, 3.
3. Fu, G.; Xu, X.; Lu, X.; Wan, H. L. (2005), *J. Am. Chem. Soc.*, *127*, 3989.
4. Mayer, J. M. (1998), *Acc. Chem. Res.*, *31*, 441.
5. Ervin, K. M. (2001), *Int. Rev. Phys. Chem.*, *20*, 127.
6. Gronert, S. (2001), *Chem. Rev*, *101*, 329.
7. Zemski, K. A.; Justes, D. R.; Castleman Jr, A. W. (2002), *J. Phys. Chem. B*, *106*, 6136.
8. Armentrout, P. B. (2003), *Eur. J. Mass Spectrom.*, *9*, 531.
9. O´Hair, R. A. J.; Khairallah, G. N. (2004), *J. Clust. Sci.*, *15*, 331.
10. O'Hair, R. A. J. (2006), *Chem. Commun.*, 1469.
11. Bohme, D. K.; Schwarz, H. (2005), *Angew. Chem. Int. Ed.*, *44*, 2336.
12. Bernhardt, T. M. (2005), *Int. J. Mass Spectrom.*, *243*, 1.
13. Cassady, C. J.; Weil, D. A.; McElvany, S. W. (1992), *J. Chem. Phys.*, *96*, 691.
14. Maleknia, S.; Brodbelt, J.; Pope, K. (1991), *J. Am. Soc. Mass Spectrom.*, *2*, 212.
15. Hachimi, A.; Poitevin, E.; Krier, G.; Muller, J. F.; Ruiz-Lopez, M. (1995), *Int. J. Mass Spectrom. Ion Processes*, *144*, 23.
16. Poels, K.; Van Vaeck, L.; Gijbels, R. (1998), *Anal. Chem.*, *70*, 504.
17. Van Vaeck, L.; Adriaens, A.; Adams, F. (1998), *Spectrochim. Acta*, *B53*, 367.
18. Aubriet, F.; Muller, J.-F. (2002), *J. Phys. Chem. A*, *106*, 6053.
19. David Jeba Singh, D. M.; Pradeep, T. (2004), *Chem. Phys. Lett.*, *395*, 351.
20. Sun, Q.; Rao, B. K.; Jena, P.; Stolcic, D.; Kim, Y. D.; Gantefor, G.; Castleman Jr, A. W. (2004), *J. Chem. Phys.*, *121*, 9417.

21. Zhai, H. J.; Huang, X.; Cui, L. F.; Li, X.; Li, J.; Wang, L. S. (2005), *J. Phys. Chem. A*, *109*, 6019.

22. Zhai, H. J.; Huang, X.; Waters, T.; Wang, X. B.; O´Hair, R. A. J.; Wedd, A. G.; Wang, L. S. (2005), *J. Phys. Chem. A*, *109*, 10512.

23. Li, S.; Dixon, D. A. (2006), *J. Phys. Chem. A*, *110*, 6231.

24. Huang, X.; Zhai, H. J.; Li, J.; Wang, L. S. (2006), *J. Phys. Chem. A*, *110*, 85.

25. Huang, X.; Zhai, H. J.; Waters, T.; Li, J.; Wang, L. S. (2006), *Angew. Chem. Int. Ed.*, *45*, 657.

26. Li, S.; Dixon, D. A. (2007), *J. Phys. Chem. A*, *111*, 11093.

27. Lau, T. C.; Wang, J.; Guevremont, R.; Siu, K. W. M. (1995), *J. Chem. Soc., Chem. Commun.*, 877.

28. Walanda, D. K.; Burns, R. C.; Lawrance, G. A.; Nagy-Felsobuki, E. I. (1999), *J. Chem. Soc., Dalton Trans.*, 311.

29. Truebenbach, C. S.; Houalla, M.; Hercules, D. M. (2000), *J. Mass Spectrom.*, *35*, 1121.

30. Deery, M. J.; Howarth, O. W.; Jennings, K. R. (1997), *J. Chem. Soc., Dalton Trans.*, 4783.

31. Bonchio, M.; Bortolini, O.; Conte, V.; Sartorel, A. (2003), *Eur. J. Inorg. Chem.*, 699.

32. Long, D. L.; Streb, C.; Song, Y. F.; Mitchell, S.; Cronin, L. (2008), *J. Am. Chem. Soc.*, *130*, 1830.

33. Schröder, D.; Engeser, M.; Brönstrup, M.; Daniel, C.; Spandl, J.; Hartl, H. (2003), *Int. J. Mass Spectrom.*, *228*, 743.

34. Feyel, S.; Schröder, D.; Schwarz, H. (2006), *J. Phys. Chem. A*, *110*, 2647.

35. Feyel, S.; Scharfenberg, L.; Daniel, C.; Hartl, H.; Schröder, D.; Schwarz, H. (2007), *J. Phys. Chem. A*, *111*, 3278.

36. Feyel, S.; Schröder, D.; Rozanska, X.; Sauer, J.; Schwarz, H. (2006), *Angew. Chem. Int. Ed.*, *45*, 4677.

37. Feyel, S.; Döbler, J.; Schröder, D.; Sauer, J.; Schwarz, H. (2006), *Angew. Chem. Int. Ed.*, *45*, 4681.

38. Day, V. W.; Klemperer, W. G. (1985), *Science*, *228*, 533.

39. Klemperer, W. G.; Wall, C. G. (1998), *Chem. Rev.*, *98*, 297.

40. Che, M.; Fournier, M.; Launay, J. P. (1979), *J. Chem. Phys.*, *71*, 1954.

41. Sanchez, C.; Livage, J.; Launay, J. P.; Fournier, M. (1983), *J. Am. Chem. Soc.*, *105*, 6817.

42. Yang, X.; Waters, T.; Wang, X. B.; O´Hair, R. A. J.; Wedd, A. G.; Li, J.; Dixon, D. A.; Wang, L. S. (2004), *J. Phys. Chem. A*, *108*, 10089.

43. Zhai, H. J.; Kiran, B.; Cui, L. F.; Li, X.; Dixon, D. A.; Wang, L. S. (2004), *J. Am. Chem. Soc.*, *126*, 16134.

44. Waters, T.; O´Hair, R. A. J.; Wedd, A. G. (2003), *J. Am. Chem. Soc.*, *125*, 3384.

45. Waters, T.; Wang, X.-B.; Li, S.; Kiran, B.; Dixon, D. A.; Wang, L. S. (2005), *J. Phys. Chem. A*, *109*, 11771.

46. Waters, T.; O´Hair, R. A. J.; Wedd, A. G. (2005), *Inorg. Chem.*, *44*, 3356.

47. Taylor, C. J.; Wu, B.; Dessent, C. E. H. (2008), *Int. J. Mass Spectrom.*, *276*, 31.

48. Fialko, E. F.; Kikhtenko, A. V.; Goncharov, V. B.; Zamaraev, K. I. (1997), *J. Phys. Chem. B*, *101*, 5772.

49. Goncharov, V. B. (2003), *Kinet. and Catal.*, *44*, 548.

50. Zhai, H. J.; Kiran, B.; Cui, L. F.; Li, X.; Dixon, D. A.; Wang, L. S. (2004), *J. Am. Chem. Soc.*, *126*, 16134.

51. Feyel, S.; Döbler, J.; Schröder, D.; Sauer, J.; Schwarz, H. (2006), *Angew. Chem. Int. Ed.*, *118*, 4797.

52. Feyel, S.; Döbler, J.; Höckendorf, R.; Beyer, M. K.; Sauer, J.; Schwarz, H. (2008), *Angew. Chem. Int. Ed.*, *47*, 1946.